

ChemComm

Accepted Manuscript



This is an *Accepted Manuscript*, which has been through the Royal Society of Chemistry peer review process and has been accepted for publication.

Accepted Manuscripts are published online shortly after acceptance, before technical editing, formatting and proof reading. Using this free service, authors can make their results available to the community, in citable form, before we publish the edited article. We will replace this *Accepted Manuscript* with the edited and formatted *Advance Article* as soon as it is available.

You can find more information about *Accepted Manuscripts* in the [Information for Authors](#).

Please note that technical editing may introduce minor changes to the text and/or graphics, which may alter content. The journal's standard [Terms & Conditions](#) and the [Ethical guidelines](#) still apply. In no event shall the Royal Society of Chemistry be held responsible for any errors or omissions in this *Accepted Manuscript* or any consequences arising from the use of any information it contains.

COMMUNICATION

Stable dispersions of azide functionalized ferromagnetic metal nanoparticles

Cite this: DOI: 10.1039/x0xx00000x

C. J. Hofer,^a V. Zlateski,^a P. R. Stoessel,^a D. Paunescu,^a E. M. Schneider,^a R. N. Grass,^a M. Zeltner^a and W. J. Stark^{*a}

Received 00th January 2012,

Accepted 00th January 2012

DOI: 10.1039/x0xx00000x

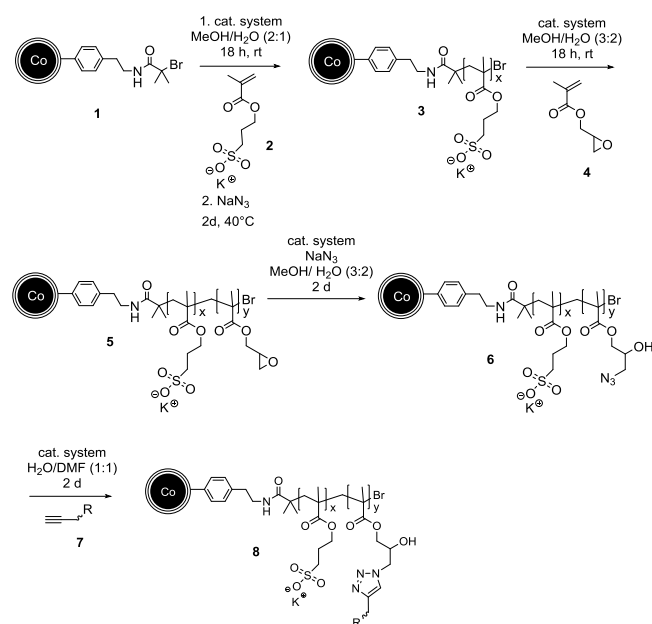
www.rsc.org/

Ferromagnetic nanoparticles are covalently modified in order to enhance the dispersion stability as well as the antifouling properties. Insertion of an azide moiety allows “click”-reaction of a relevant tag molecule. This and the high saturation magnetization of the presented nanocomposite offer a promising platform for magnetic biosensors.

Since the commercial implementation of blood glucose monitoring devices for diabetes patients or pregnancy tests, biosensors were accepted as a fast and reliable high-end analytical method.¹ In addition to optically based detection methods, target molecules could also be detected and quantified by magnetically based techniques.² For these applications nano-sized magnetic particles³ seem to be most promising.⁴ In case of medical diagnostic systems the requirements for particles include dispersability in aqueous solution, uniformity of particle sizes, minimization of unspecific binding (biofouling) and high saturation magnetization. Furthermore, an efficient method for the attachment of biomolecules to the surface of the magnetic labels is crucial.⁵ Ferromagnetic pure metallic nanomagnets (*e.g.* carbon coated cobalt nanoparticles (C/Co))⁶ show a substantially higher saturation magnetization compared to the often used superparamagnetic iron oxide nanoparticles⁷, making them a promising candidate for biosensing applications. However, these ferromagnetic nanoparticles usually exhibit several drawbacks for biological or bio-medical applications namely their inferior dispersion stability (formation of agglomerates) in biological relevant solvents, their high unspecific binding tendency with proteins due to their hydrophobic surface and the difficulty of reliably attaching a desired molecule. This creates an urgent need for a material, which combines the advantageous properties of ferro- (high saturation magnetization) and superparamagnetic (dispersion stability) nanoparticles. Polymer coating of particles allow achieving this goal by building a defined organic layer on the inorganic core.⁸ This organic layer not only gives new surface properties to the organic-inorganic colloids and

therefore changes the particle properties (in terms of hydrophilicity, aggregation tendency *etc.*) but also gives the particles the processability of a polymer.⁹ Installation of polymer coatings can be done in various ways and can be grouped into *in situ* coatings and post-synthesis coatings.¹⁰ The post-synthesis coating method consists of grafting the polymer on the magnetic particles after synthesis. An often used method is polymer growth from the particles surface by atom transfer radical polymerization (ATRP) as a “grafting from” approach.⁹ A key advantage of this controlled radical polymerization is the possibility to achieve well-defined polymers in terms of thickness and composition. Post-modification of the polymer layer enables introduction of various chemical functionalities for instance via active esters, Diels-Alder cycloaddition, Michael addition, thiol-ene addition, epoxides, isocyanates, copper-catalyzed azide-alkyne cycloaddition (CuAAC) and combinations of them.¹¹ Here, we describe the formation of a ferromagnetic nanocomposite with unprecedented dispersion stability and enhanced antifouling properties by specific “grafting from” surface modification with a covalently attached, negatively charged block-copolymer. Post-modification of this material by the well-known “click”-reaction¹², allows the attachment of various desired target molecules. These properties enable applications of this highly demanded magnetic platform for biosensor applications.

The ferromagnetic particles presented here are based on carbon coated cobalt nanoparticles. They are composed of a metal core and thin graphene-like protection layers (ca. 1 nm) which allow covalent attachment of a broad scope of functional groups to the surface.⁶ The synthesis of this dispersion-stable, ferromagnetic nanocomposite is shown in Scheme 1. After covalent implementation of a starter-moiety for surface initiated atom transfer radical polymerization (SI-ATRP) to the C/Co-particles (C/Co@initiator **1**),¹³ negatively charged 3-sulfopropyl methacrylate (SPM, **2**) was polymerized to the particles to yield C/Co@pSPM (**3**). The covalent nature of the binding prevents detachment of the polymer strands, as it possibly occurs in the case



Scheme 1: Covalent functionalization of carbon coated cobalt nanoparticles. Diazonium chemistry and amidation were used to generate C/Co@initiator (1) for SI-ATRP of 3-sulfopropyl methacrylate potassium salt (SPM, 2) to yield C/Co@pSPM (3). Glycidyl methacrylate (GMA, 4) was copolymerized to C/Co@pSPM (3) to obtain C/Co@pSPM-b-pGMA (5). Azide functionality was introduced by epoxide ring-opening to yield C/Co@pSPM-N₃ (6). Different molecules obtaining a propargyl group (7) can be coupled to the magnetic nanoparticles by copper-catalyzed-azide-alkyne cycloaddition (CuAAC) to obtain C/Co@pSPM-clicked (8). Catalytic system: copper(II)bromide (CuBr₂), 2,2'-bipyridine, L-ascorbic acid.

of physisorption. The polymer helps to stabilize dispersions and to avoid aggregation by steric hindrance and electrostatic charge repulsion as previously shown for charged coating.¹³ Longer SPM-polymer chains afford a better colloidal stability, but lower the overall magnetization of the material (see equation S1). This opens the possibility to tune the particle properties concerning colloidal stability and overall magnetization specifically for a given application. Usage of too short polymers (less than 6 SPM units) resulted in unstable dispersions as measured by sedimentation analysis using analytical centrifugation (see Fig. 1, Table S3, S4 and Fig. S10). Moreover, the negatively charged polymer SPM is known for its antifouling properties under relevant aqueous conditions.¹⁴ In order to couple a molecule of interest to the magnetic nanocomposite, copper-catalyzed azide-alkyne cycloaddition (CuAAC), also known as "click"-reaction, was chosen as one of the most often used coupling systems in biochemistry (mild conditions, high yields).¹⁵ Attempts to directly substitute the bromine end-group of C/Co@pSPM (3) by azide, failed possibly due to charge repulsion between SPM and the azide ion. Glycidyl methacrylate (GMA, 4) was therefore polymerized onto C/Co@pSPM (3) to generate the block-copolymer C/Co@pSPM-b-pGMA (5). The GMA unit offers the possibility of post-modification in order to insert the azide by epoxide ring-opening, as previously shown.¹⁶ By standard "click"-chemistry a desired substrate linked with an alkyne (7) can be reliably attached to the magnetic composite beads. Particles were washed after each reaction step by magnetic decantation of the reaction solvent and redispersion in different solvents. Then they were dried *in vacuo* (see Fig. S4). All reaction

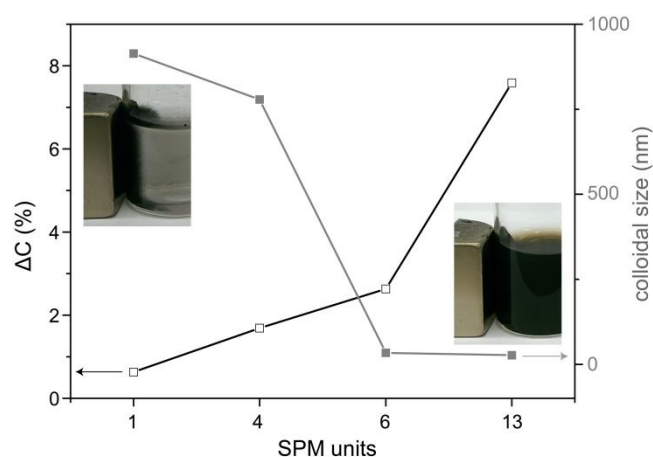


Fig. 1: Carbon content increase after SPM polymerization measured by elemental microanalysis and colloidal size in water measured by sedimentation analysis using analytical centrifugation of C/Co@pSPM (3) containing different amounts of SPM units per ATRP initiator. It is clearly observable that colloidal stability correlates with polymer chain length. Colloidal stability is reached at a chain length of about 6 SPM units per ATRP initiator.

steps were analysed by Fourier transform infrared spectroscopy (FT-IR) (see Fig. S5) and elemental microanalysis (see Table S1 for results and discussion). Incorporation of the azide moiety in C/Co@pSPM-N₃ (6) was confirmed by the characteristic azide-vibration peak appearing at 2108 cm⁻¹. The successful coupling of a propargyl derivative (using the example of biotin-PEG₄-alkyne) was confirmed by the decline of this azide-vibration peak and the appearance of new peaks corresponding to the amid-, urea-, and polyethyleneglycol-part of the coupled biotin-PEG₄-alkyne (see Fig. S5). We furthermore quantitatively characterized some key intermediates of our material by thermal gravimetric analysis (see Fig. S1-S3). By comparing the scanning transmission electron micrographs (STEM) of non-functionalized and functionalized cobalt nanocomposites, it can be observed that the functionalized particles are clearly separated from each other while the non-modified nanoparticles stick together and form aggregates (Fig. 2a) and b)). These findings indicate that the covalently attached polymer brushes indeed grew from the surface (see also Fig. S7 for STEM pictures of 3)¹³. Average particles size of C/Co@pSPM-clicked (8), determined by optical diameter analysis, is 27 ± 19 nm (measured from STEM Fig. S8). Successful polymerization was additionally confirmed by transmission electron microscopy (TEM), where the coating surrounding the metal core is clearly visible (Fig. 2c).

As mentioned before, dispersion stability in relevant solvents is one of the key properties of nanoparticles in bio-medical applications.⁵ The functionalized particles C/Co@pSPM (3) are not only substantially more stable compared to the non-modified particles in water but also in biologically relevant phosphate buffered saline (PBS), PBS with dissolved albumin (50 mg/mL) and Eagle's minimal essential medium (DMEM) (Fig. 3). Negative polymer charge is essentially necessary, as particles coated with cationic poly[3-(methacryloyl amino)propyl] trimethylammonium chloride (pMAPTAC)¹³ lack this stability in aqueous buffer and cell-medium. Conclusion about dispersion stability can also be drawn from particle size distribution measurements using analytical centrifugation. An average

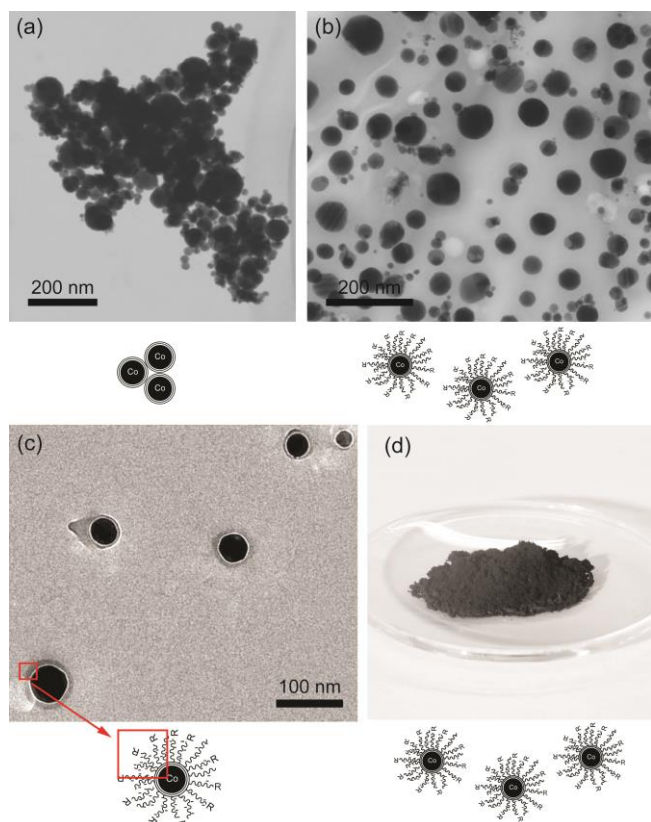


Fig. 2: Scanning transmission electron micrographs (STEM) of (a) non-functionalized C/Co and (b) C/Co@pSPM-clicked (**3**). The coated nanoparticles show clear separation of the individual nanoparticles. The transmission electron micrograph (TEM) of C/Co@pSPM-clicked (**3**) (c) shows again the separation as well as the polymer layer surrounding the metal core. Nanopowder of C/Co@pSPM (**3**) is shown in (d).

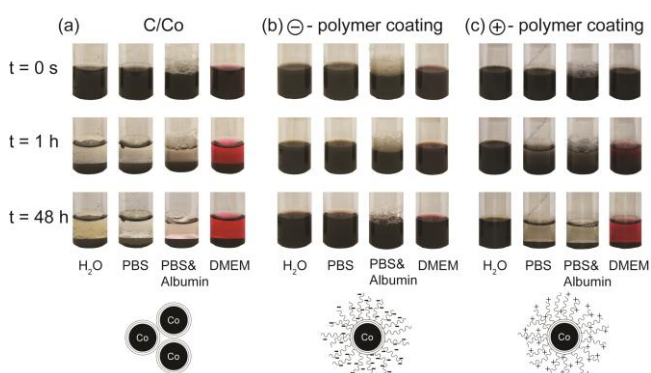


Fig. 3: Stability test of dispersions of non-functionalized C/Co-nanoparticles (a), C/Co@pSPM (**3**) (b) and positively charged pMAPTAC coated C/Co-nanoparticles (**3**) (c) in different media at a concentration of 1 mg/mL. The non-functionalized particles completely settled after 1 h while the nanoparticles containing covalently coated negatively charged polymer (**3**) still form stable dispersions after 48 h in all media. Poly[3-(methacryloyl amino)propyl] trimethylammonium chloride (pMAPTAC) coated particles show enhanced stability in water but lack this stability in buffer and cell-medium.

hydrodynamic particle size of around 35 nm for C/Co@pSPM-N₃ (**6**) in four different media (H₂O, PBS, PBS with albumin and DMEM) was found (see Table S2 for sedimentation analysis results of analytical centrifugation of **3** and **6**). This suggests good dispersion stability in

all media. In addition, dynamic light scattering (DLS) measurements of C/Co@pSPM (**3**) and C/Co@pSPM-N₃ (**6**) in water over 24 minutes showed no cluster growth (see Table S6). As the stability in dispersion directly correlates to the surface potential, the zeta potential gives additional evidence for the dispersion stability.¹⁷ Comparing the particles following the reaction path direction from C/Co to C/Co@pSPM-N₃ (**6**), the highest zeta potential (-47 ± 6 mV) is observed for C/Co@pSPM (**3**) (Fig. 4). After insertion of the non-charged GMA as a block-copolymer and post-modification with azide, the negative charge of poly(SPM) is shielded to some extent and the zeta potential of C/Co@pSPM-N₃ (**6**) is reduced to -26 ± 4 mV. However, the complete functionalized nanoparticles C/Co@pSPM-N₃ (**6**) still show a zeta potential higher than non-functionalized superparamagnetic nanoparticles. Ferromagnetic C/Co feature higher saturation magnetization (151 emu g^{-1})⁶ than the iron oxide counterpart (max. $92^{18} \text{ emu g}^{-1}$, depending on synthesis route¹⁹). In both cases the saturation magnetization per gram particles is lowered by the coating process (as coating involves mass gain).²⁰ However, the azide functionalized cobalt nanoparticles C/Co@pSPM-N₃ (**6**) still possess a saturation magnetization (93 emu g^{-1}) in the range of non-functionalized iron oxide (see Fig. S11 for plots of magnetic hysteresis susceptibility of C/Co, **3** and **6**) while the saturation magnetisation of commercial dextran-coated iron oxide nanoparticles drops to 7 emu g^{-1} of particles (Fig. 4). This low magnetization level makes magnetic detection and movement by application of a magnetic field difficult.^{21,20}

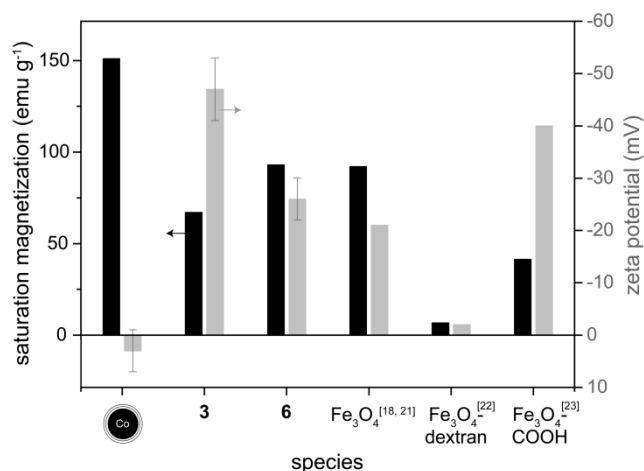


Fig. 4: Saturation magnetization (black) and zeta potential (grey) of non-functionalized C/Co nanoparticles, C/Co@pSPM (**3**), C/Co@pSPM-N₃ (**6**) and different commercially available reference materials (plain iron oxide nanoparticles (Fe₃O₄), dextran-coated iron oxide nanoparticles (Fe₃O₄-dextran) and carboxylic acid functionalized iron oxide nanoparticles (Fe₃O₄-COOH)).

As mentioned above, the antifouling nature of the nanoparticle surface is important in biosensing applications. SPM-polymers bear the potential to avoid or reduce fouling as shown elsewhere.¹⁴ The fouling properties of the developed particles and some reference materials were investigated by adsorption of the enzyme β -glucosidase from almonds on the nanoparticles.²⁴ To quantify the amount of adsorbed enzyme, the enzyme activity of the remaining supernatant was measured. This was done by measuring the absorbance of the hydrolysis product of 4-nitrophenyl β -D-

glucopyranoside by β -glucosidase, which is nitrophenol. The absorbance of nitrophenol was measured as a function of enzyme exposure time. As shown in Fig. S13 the biofouling tendency of C/Co@pSPM (**3**) was lowered by 70% compared to non-functionalized C/Co and therefore has similar fouling tendency as silica particles but slightly higher than dextran or polyethylene glycol (PEG)-coated iron oxide nanoparticles. Insertion of azide moieties in C/Co@pSPM-N₃ (**6**) decreased the antifouling properties compared to C/Co@pSPM (**3**).

In conclusion we demonstrate the development of novel carbon coated cobalt nanoparticles with covalent azide-functionality and high stability in aqueous dispersions. The high stability in dispersion was achieved by covalent grafting of anionic 3-sulfopropyl methacrylate from the graphene-like layers surrounding the metal core by SI-ATRP. The subsequent formation of a block-copolymer with GMA and post-modification enabled the introduction of azide functionality. The proposed synthesis route allows the attachment of various target molecules to the magnetic beads by "click"-chemistry. The unspecific binding of proteins with functionalized carbon coated cobalt nanoparticles was more than halved compared to their non-functionalized equivalent (C/Co) and remains in the same range as for silica particles. The magnetization of the developed coated nanoparticles C/Co@pSPM-N₃ (**6**) compared to the commercial coated magnetite nanoparticles was substantially higher (ranging from 2 (for Fe₃O₄-COOH) to 14 times (for Fe₃O₄-dextran)). Thus, this material provides a promising platform for magnetic detection based biosensors and other applications.

Financial support was provided by ETH Zurich, the EU/ITN network Mag(net)icfun (PITN-GA-2012-290248) and the Swiss National Science Foundation (no. 200021-150179).

Notes and references

^a Institute for Chemical and Bioengineering at the Swiss Federal Institute of Technology Zurich, CH-8093 Zurich, Switzerland. Tel.: +41 44 632 0980. E-mail: wendelin.stark@chem.ethz.ch

The authors declare the following competing financial interest(s): Two authors (W.J.S. and R.N.G.) declare financial interests, as they are shareholders of TurboBeads LLC, a company active in magnetic nanoparticles.

† Electronic Supplementary Information (ESI) available: experimental details, FT-IR spectra, elemental analysis, additional STEM pictures, data of sedimentation analysis by analytical centrifugation, magnetic hysteresis susceptibility (VSM) results, antifouling test and calculations are attached.

See DOI: 10.1039/c000000x/

- (a) *Br. Pat.*, 2 051 360, 1980; (b) *Br. Pat.*, 2 204 398, 1988
- (a) D. L. Graham, H. Ferreira, J. Bernardo, P. P. Freitas and J. M. S. Cabral, *J. Appl. Phys.*, 2002, **91**, 7786; (b) J. Richardson, A. Hill, R. Luxton and P. Hawkins, *Biosens. Bioelectron.*, 2001, **16**, 1127; (c) P. I. Nikitin, P. M. Vetoshko and T. I. Ksenevich, *J. Magn. Magn. Mater.*, 2007, **311**, 445; (d) S. Lee, W. R. Myers, H. L. Grossman, H. M. Cho, Y. R. Chemla and J. Clarke, *Appl. Phys. Lett.*, 2002, **81**, 3094; (e) D. R. Baselt, G. U. Lee, K. M. Hansen, L. A. Chrisey and R. J. Colton, *Proc. IEEE*, 1997, **85**, 672; (f) S. Katsura, T. Yasuda, K. Hirano, A. Mizuno and S. Tanaka, *Supercond. Sci. Technol.*, 2001, **14**, 1131; (g) K. Enpuku, T. Minotani, T. Gima, Y. Kuroki, Y. Itoh, M. Yamashita, Y. Katakura and S. Kuhara, *Jpn. J. Appl. Phys. Part 2 - Lett.*, 1999, **38**, L1102; (h) P. A. Besse, G. Boero, M. Demierre, V. Pott and R. Popovic, *Appl. Phys. Lett.*, 2002, **80**, 4199; (i) M. M. Miller, G. A. Prinz, S. F. Cheng and S. Bounnak, *Appl. Phys. Lett.*, 2002, **81**, 2211; (j) J. C. Rife, M. M. Miller, P. E. Sheehan, C. R. Tamanaha, M. Tondra and L. J. Whitman, *Sens. Actuator A-Phys.*, 2003, **107**, 209; (k) D. R. Baselt, G. U. Lee, M. Natesan, S. W. Metzger, P. E. Sheehan and R. J. Colton, *Biosens. Bioelectron.*, 1998, **13**, 731.
- A. H. Lu, E. L. Salabas and F. Schuth, *Angew. Chem.-Int. Edit.*, 2007, **46**, 1222.
- (a) E. Alphantery, L. Lijeour, Y. Lalatonne and L. Motte, *Sens. Actuator B-Chem.*, 2010, **147**, 786; (b) J. B. Haun, T. J. Yoon, H. Lee and R. Weissleder, *Wiley Interdiscip. Rev.-Nanomed. Nanobiotechnol.*, 2010, **2**, 291; (c) I. Koh and L. Josephson, *Sensors*, 2009, **9**, 8130; (d) S. X. Wang and G. Li, *IEEE Trans. Magn.*, 2008, **44**, 1687.
- A. Sandhu, H. Handa and M. Abe, *Nanotechnology*, 2010, **21**, 22.
- R. N. Grass, E. K. Athanassiou and W. J. Stark, *Angew. Chem.-Int. Edit.*, 2007, **46**, 4909.
- T. Osaka, T. Matsunaga, T. Nakanishi, A. Arakaki, D. Niwa and H. Iida, *Anal. Bioanal. Chem.*, 2006, **384**, 593.
- A. K. Gupta and M. Gupta, *Biomaterials*, 2005, **26**, 3995.
- E. Bourgeat-Lami, *J. Nanosci. Nanotechnol.*, 2002, **2**, 1.
- S. Laurent, D. Forge, M. Port, A. Roch, C. Robic, L. V. Elst and R. N. Muller, *Chem. Rev.*, 2008, **108**, 2064.
- M. A. Gauthier, M. I. Gibson and H. A. Klok, *Angew. Chem.-Int. Edit.*, 2009, **48**, 48.
- H. C. Kolb, M. G. Finn and K. B. Sharpless, *Angew. Chem.-Int. Edit.*, 2001, **40**, 2004.
- M. Zeltner, R. N. Grass, A. Schaetz, S. B. Bubenhofer, N. A. Luechinger and W. J. Stark, *J. Mater. Chem.*, 2012, **22**, 12064.
- (a) M. Kobayashi, Y. Terayama, H. Yamaguchi, M. Terada, D. Murakami, K. Ishihara and A. Takahara, *Langmuir*, 2012, **28**, 7212; (b) F. Wan, X. W. Pei, B. Yu, Q. Ye, F. Zhou and Q. J. Xue, *ACS Appl. Mater. Interfaces*, 2012, **4**, 4557.
- J. M. Baskin and C. R. Bertozzi, *QSAR Comb. Sci.*, 2007, **26**, 1211.
- W. W. He, L. Cheng, L. F. Zhang, X. W. Jiang, Z. Liu, Z. P. Cheng and X. L. Zhu, *Nanotechnology*, 2014, **25**, 11.
- R. Greenwood and K. Kendall, *J. European Ceram. Soc.*, 1999, **19**, 479.
- C. J. Goss, *Phys. Chem. Miner.*, 1988, **16**, 164.
- G. F. Goya, T. S. Berquo, F. C. Fonseca and M. P. Morales, *J. Appl. Phys.*, 2003, **94**, 3520.
- Y. Yuan, D. Rende, C. L. Altan, S. Bucak, R. Ozisik and D. A. Borca-Tasciuc, *Langmuir*, 2012, **28**, 13051.
- M. Mahmoudi, A. Simchi, M. Imani, M. A. Shokrgozard, A. S. Milani, U. O. Hafeli and P. Stroeve, *Colloid Surf. B-Biointerfaces*, 2010, **75**, 300.
- Oceannanotech, <http://www.oceannanotech.com/product.php?cid=69&pid=122>, (accessed August 2014).
- (a) Oceannanotech, <http://www.oceannanotech.com/product.php?cid=69&pid=151>, (accessed August 2014); (b) Micromod Partikeltechnologie GmbH, http://www.micromod.de/pdf/aktuell/79-00-501_tds_en.pdf, (accessed August 2014).
- V. Zlateski, R. Fuhrer, F. M. Koehler, S. Wharry, M. Zeltner, W. J. Stark, T. S. Moody and R. N. Grass, *Bioconjugate Chem.*, 2014, **25**, 677.